Energy dependence of total cross sections of $D^*(2010)$ mesons on HERA colider

Nataliia Zakharchuk
National University Kyiv-Mohyla Academy, Ukraine

DESY ZEUS Group

11th Jule 2012, Hamburg

Abstract

The energy dependence of the total cross section of $D^{*\pm}(2010)$ mesons with three different proton beam energies: High Energy Range - 920 GeV, Middle Energy Range - 575 GeV, Low Energy Range - 460 GeV in electron proton collisions at the HERA is presented in this report. The analysed data were collected with ZEUS detector during 2006-2007 which correspond to an integrated luminosity of $L_{HER} = 159.9pb^{-1}$, $L_{MER} = 7.77pb^{-1}$, $L_{LER} = 13.18pb^{-1}$. Charm production events were identified by reconstruction of D^* mesons in the $D^*(2010) \to D^0, \pi_s \to K, \pi, \pi_s$ decay channel. In the restricted phase space 20 GeV $> p_T(D^*) >$ 1.9 GeV, $|\eta(D^*)| < 1.6$, 130 GeV $< W_{HER} <$ 285 GeV, 100 GeV$< W_{MER} <$ 235 GeV, 85 GeV$< W_{LER} <$ 205 GeV the total cross section was measured to $\sigma^{HER}_{total} = 31773 \pm 616(stat)pb^{-1}$, $\sigma^{MER}_{total} = 26127 \pm 2612(stat)pb^{-1}$, $\sigma^{LER}_{total} = 23536 \pm 1923(stat)pb^{-1}$ and the observed energy dependence of total cross sections.

Contents

1 Motivation

Main goal of this analysis is measure energy dependence visible of cross section of $D^*(2010)$ mesons in electron-proton interaction for $D^*(2010) \to D^0, \pi_s \to K, \pi, \pi_s$ decay channel in PHP.

This results will be first investigation in ZEUS collaboration and are interest about theoretical predictions - FMNAR.

2 Introduction

On HERA machine collided electrons and positrons, accelerated to an energy of 27.5 GeV, with 920 GeV protons (also were periods with two different proton energies 460 GeV (Low Energy Run) and 575 Gev (Medium Energy Run)).

The *ep* scattering phase space is subdivided into two regions: for Q^2>1 GeV^2 processes are reffered as *Deep Inelastic Scattering (DIS)*. Events with Q^2<1 GeV^2 are called *Photoproduction (PHP)*.

In analysis consider photoproduction (PHP) processes, which include D^* mesons. In photoproduction processes at HERA, a quasi - real photon (Q^2=0) is emitted by the incoming electron or positron, and interacts with the proton. There are two types photoproduction:

- *direct processes*, where the photon participates as a point-like particle interacting with the gluon from the photon and giving $c\bar{c}$ pair.

- *resolved processes*, where the photon behaves as a source of partons which can scatter off the partons in the proton (see Fig.1.1.)

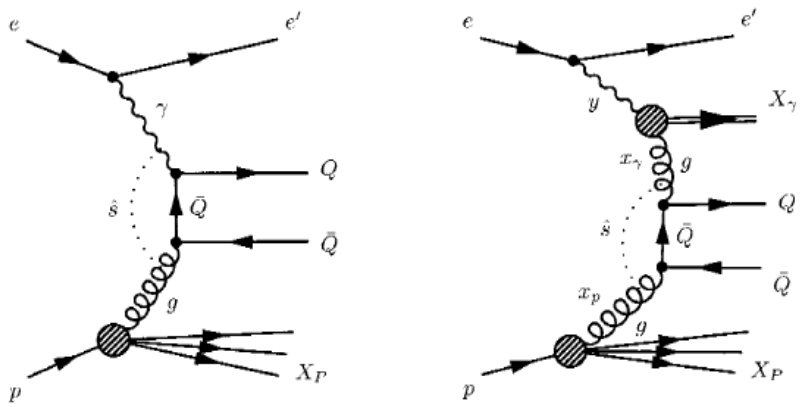

Figure 2.1: Diagram a) direct process b)resolved process

In limits PHP process reconstracted such processes: $e^{\pm}+p \Rightarrow \gamma+g(\gamma \to g+X) \Rightarrow$ hadronisation $\Rightarrow D^* \to D^0, \pi_s \to K, \pi, \pi_s$.

This decay channel has essential advantages, despite small probability ($2.6 \pm 0.5\%$):

- Three daughter particles in the final state give a possibility for better selection of events.

- The small differences in mass between $\Delta M = 145.5 \pm 0.6$ MeV and $M(\pi^{\pm}) =$ 139.6 MeV yields a low momentum pion from the D^* decay and prominent signals just above the threshold of the $((K\pi\pi_s) - (K\pi)$, where the phase space contribution is highly suppressed.

- High and narrow peak allows to easily distinguish a background.

3 D^* observation

3.1 Reconstruction of kinematic variables

On the initial stage for separating events is to aplly restrictions on the kinematic variables. For the reconstruction of kinematic variables in this analysis used *Jacquet-Blondel method.*

He is applied in photoproduction, when the interacting electron is absent or undetected being scattered at low angle down into the beam pipe.The event kinematics can also be reconstructed using only the hadronic final state variables δ_{had} and $p_{T,had}$:

$$\delta_{had} = E_{had} - p_{z,had}$$

$$Q_{JB} = \frac{p^2_{T,had}}{1 - y_{Jb}},$$

$$y_{JB} = \frac{\delta_{had}}{2E_e},$$

$$x_{JB} = \frac{Q_{JB}}{s y_{JB}},$$

$$W_{JB} = \sqrt{s \cdot y_{JB}}.$$

3.2 D^* meson selection and reconstruction

3.2.1 Data selection

For the reconstruction D^* mesons is necessary that the event passed triggers:

- **HFL01** triggers - selection of events Photoproduction;
- **HFM01** triggers if D^* candidate decaying in the channel $D^*(2010) \to D^0, \pi_s \to K, \pi, \pi_s$.

The following selection for photoproduction events has been applied:

- Electron energy and probability cut.

  We require to have no good SINISTRA electron with probability electron > 0.9 and electron energy $E_e > 5$ GeV.

- 130 $GeV < W_{HER} <$ 285 GeV

  100 $GeV < W_{MER} <$ 235 GeV

  85 $GeV < W_{LER} <$ 205 GeV,

  where W is the Jacquet-Blondel estimators.

The following the track cuts that are used in the reconstruction of D^* candidates:

- $|\eta\ (D^*)| < 1.6$: the kinematic region in the pseudorapidity of D^*, corresponding to a range of polar angle 23° - 157°
- $|\eta\ (K, \pi, \pi_s)| < 1.7$:the kinematic region in the pseudorapidity of daughter particles, corresponding to a range of polar angle 20^o - 160°
- 1.9 GeV $< P_t\ (D^*) <$ 20 GeV: the kinematic region in D^* transverse momenta
- $P_t\ (K, \pi) > 0.4$ GeV: the cuts on kaon and pion track transverse momenta
- $P_t\ (\pi_s) > 0.12$ GeV: the cuts on pion "slow" track transverse momenta
- $\frac{P_t}{E_t} > 0.12$
- 1.83 GeV $< M(D^0) <$ 1.90 GeV range for the invariant mass of the pion and kaon of the D^0 meson candidate (see Fig.2.1)
- $P_t(\pi_s)$ - corrections (0.1<pt<0.26: 1.+0.548(pt-0.26); pt>0.26: 1)

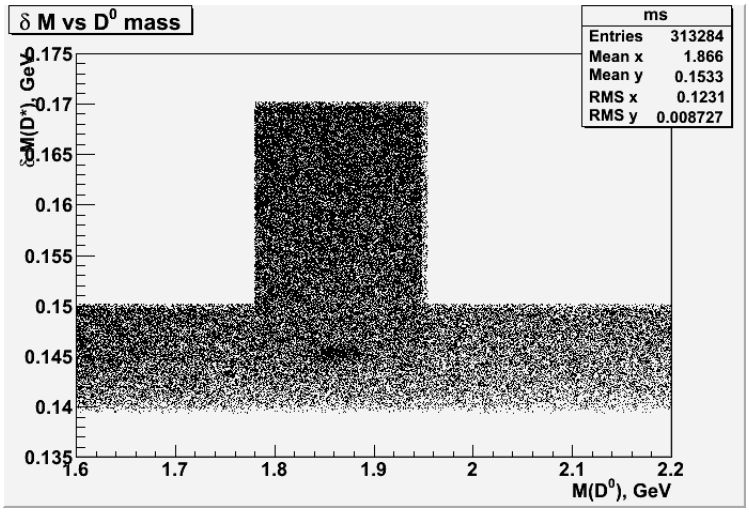

Figure 3.1: Distributions of mass $M(D^0)$ vs $(M(D^*) - M(D^0))$(8400000 events). Clearly shows the limits for $M(D^0)$.

3.2.2 Monte Carlo selection

In this analysis used Pythia inclusive charm in photoproduction Monte Carlo sample for HER. It contains information about primary conditions of particles and their decay products. The integrated luminosity is the same to the date. For MER and LER used Pythia inclusive charm in photoproduction Monte Carlo sample with D^* filter.

The following selection events has been applied:

- Q^2<1
- $|\eta(D^*)| < 1.6$
- 20 GeV $> p_T(D^*) >$ 1.9 GeV

Do not apply restrictions on the daughter particles and look for D^* candidate. In Monte Carlo they have found. Information about them can be found in MCDSTAR block.

3.3 Mass distributions

The ΔM distributions of channel $D^*(2010) \rightarrow D^0, \pi_s \rightarrow K, \pi, \pi_s$ for different energies are shown in Figure 2.2.

D^* reconstruction relies entirely on combining all possible track configurations from tracks that confirm to the requirements listed in the previous section. This procedure creates a large number of meaningless background combinations that arise from random track configurations that must be accounted for and removed. Combinatorial background is significant and accounts for around half of the total candidates in the signal region.

Background is estimated by storing D^* candidates constructed from wrong charge track combinations corresponding to unphysical particles and which have a mathematically identical shape to the background in the ΔM distributions. To count the number of reconstructed D^*'s the wrong-charge background must be subtracted from the right-charge candidates.

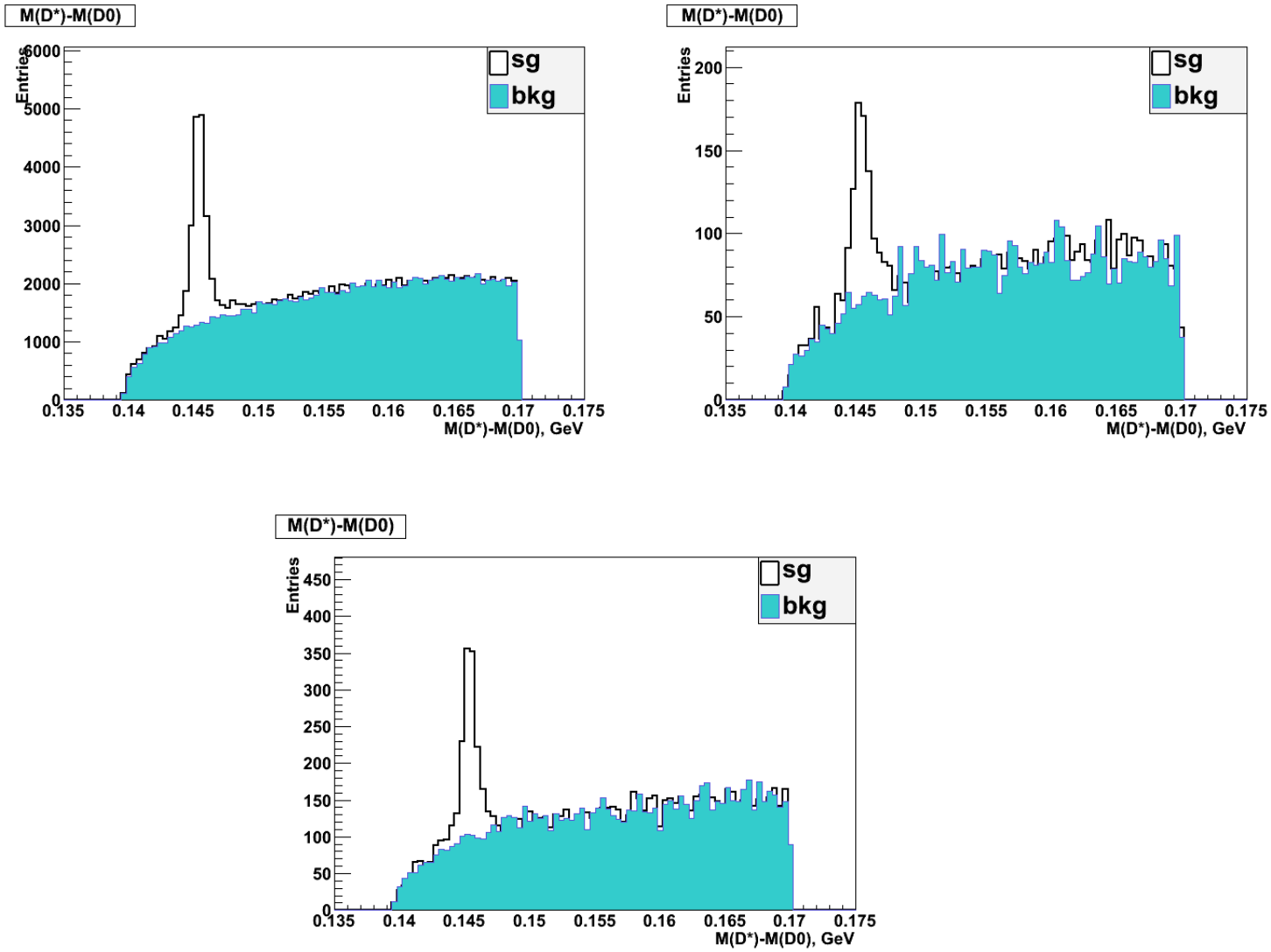

Figure 3.2: ΔM distribution for D^* candidates with the corresponding wrong charge distribution (blue color) for HER, MER, LER.

The number of D^* can be calculated with next formula

$$N(D^*) = A - B \cdot k$$

where $k = C/D$ - coefficient of normalization

The error associated with this number are calculated as follows:

$$\delta(N) = \sqrt{(A + \frac{1}{D^2}\{BC(B + C + \frac{BC}{D}).}$$

To calculate the amount of D^* can be introduce the following notation:

- **[A]** - the number of D^* mesons in the region $\delta M \in [143.5; 147.5]$ MeV in signal;
- **[B]** - the number of D^* mesons in the region $\delta M \in [143.5; 147.5]$ MeV in background;
- **[C]** - the number of D^* mesons in the region $\delta M \in [150; 167]$ MeV in signal;
- **[D]** - the number of D^* mesons in the region $\delta M \in [150; 167]$ MeV in background;

Figure 2.3 identifies the signal and background regions of ΔM and assigns relevant labels. The number of D^*'s in the signal region for the right charge combination candidates is A and the number in the background normalisation region is B. The corresponding labels for the wrong charge candidates are C and D for the signal and background regions respectively.

The number of D^* mesons reconstructed using this method are shown in Table 1.

Table 1: Number of D^* mesons

Periods	$N(D^*)$ DATA	$N(D^*)$ MC
2006-07p,HER	12850 ± 212	13783 ± 140
2006-07p,MER	538 ± 44	417 ± 23
2006-07p,LER	948 ± 58	461 ± 24

In the Figure 2.4 shows that the combinatorial background for the Monte Carlo lower in comparison with real data. The number of reconstructed particles is calculated in the same way as for real data.

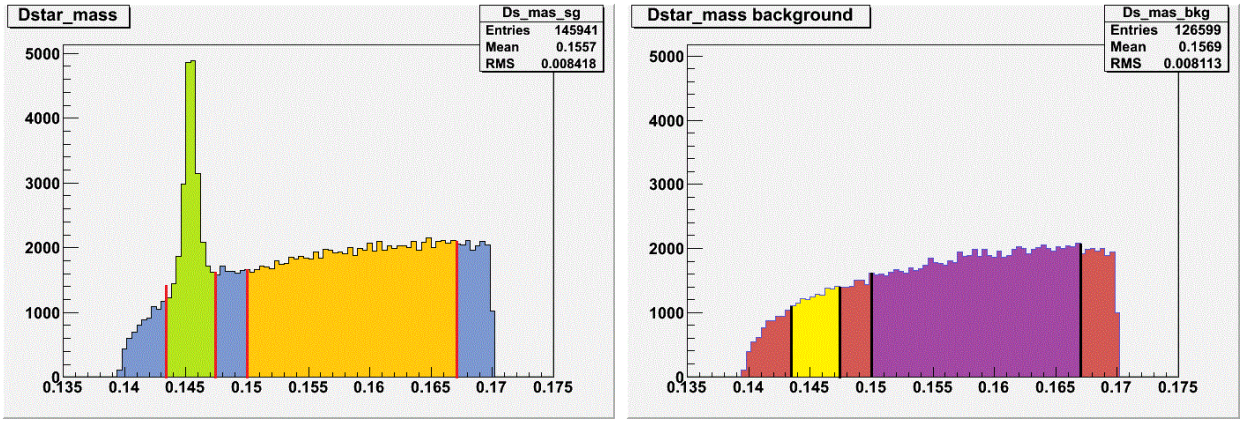

Figure 3.3: Illustration of the signal and background regions of the left and wrong charge combinations (right) of D^* candidates.

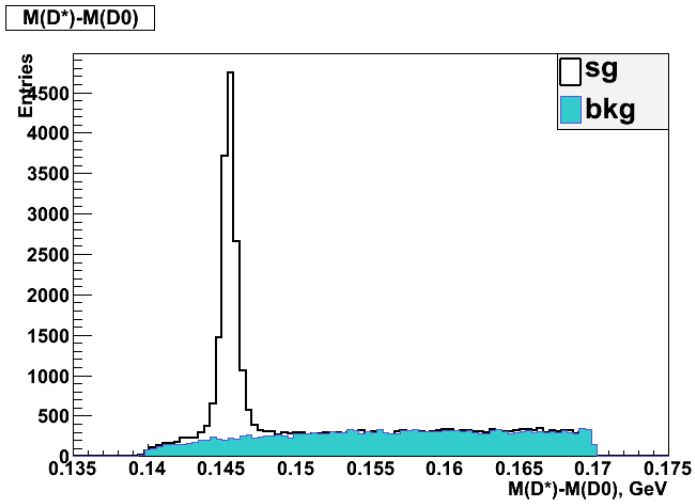

Figure 3.4: Distributions of $\delta M(D^*)$ for MC (HER)

4 Comparison CN v06a and v07a

Comparison CN v06a and v07a are present in this chapter. Mass distribution for each versions are shown in Figure 3.1 and the number of D^* mesons are calculated in Table.2.

Table 2: Number of D^* mesons

Periods	$N(D^*)$ v06a	$N(D^*)$ v07a
06/07p,HER	12850 ± 212	13513 ± 221
07p,MER	538 ± 44	562 ± 46
07p,LER	948 ± 58	953 ± 61

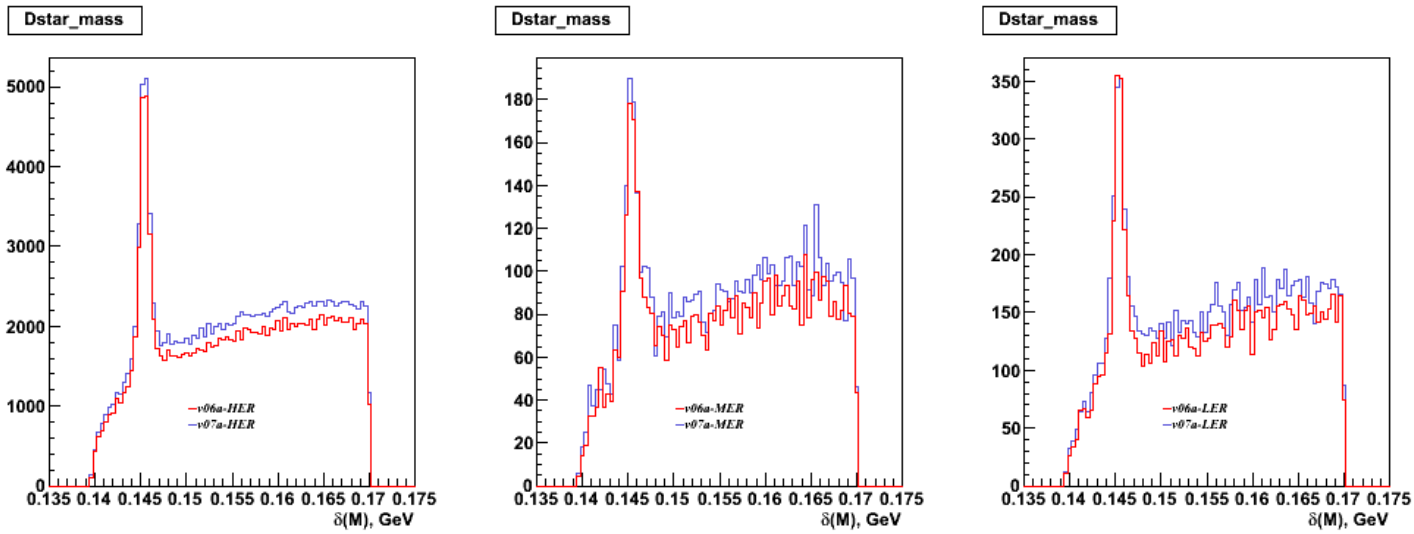

Figure 4.1: Distributions of $\delta M(D^*)$ signals for for different energy.

Check of kinematic variables are shown in the Figure.3.2-3.4.

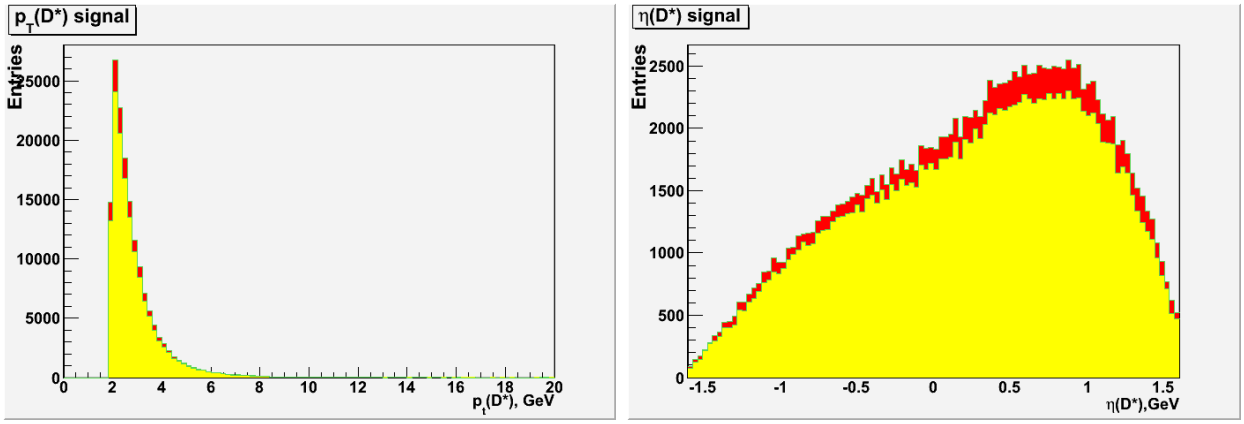

Figure 4.2: Comparison of distributions $\eta(D*)$ and $p_T(D*)$ for HER (red-v07a, yellow-v06a).

There are statistics calculated for each period (see in Table 3).

Table 3: Statistics for each energy.

E_p	v07a	v06a	v06a/v07a	difference
HER	160824	145941	0,91	9%
MER	6989	6221	0,89	11%
LER	11850	10580	0.89	11%

The distributions are similary. New version Common Ntuple has approximately

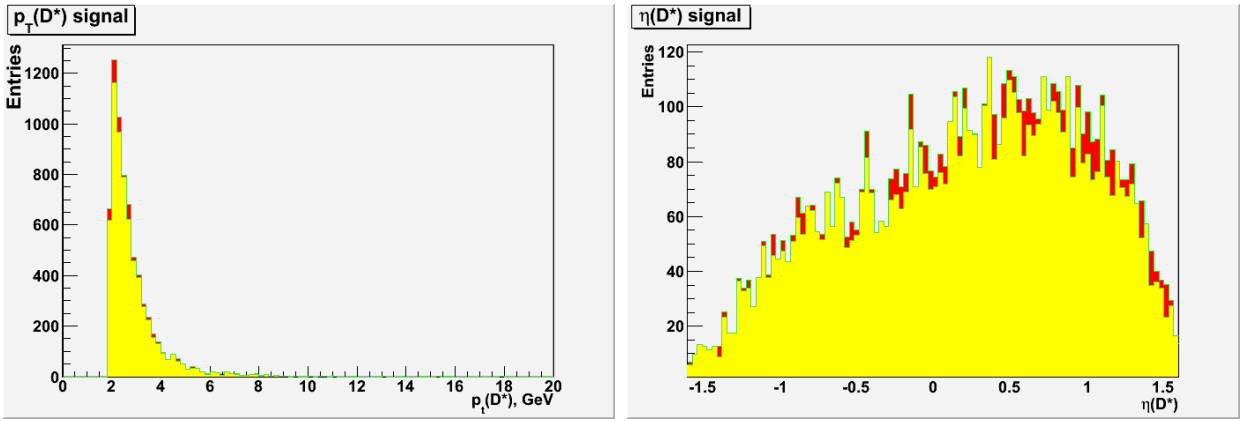

Figure 4.3: Comparison of distributions for $\eta(D*)$ and $p_T(D*)$ for MER (red-v07a, yellow-v06a).

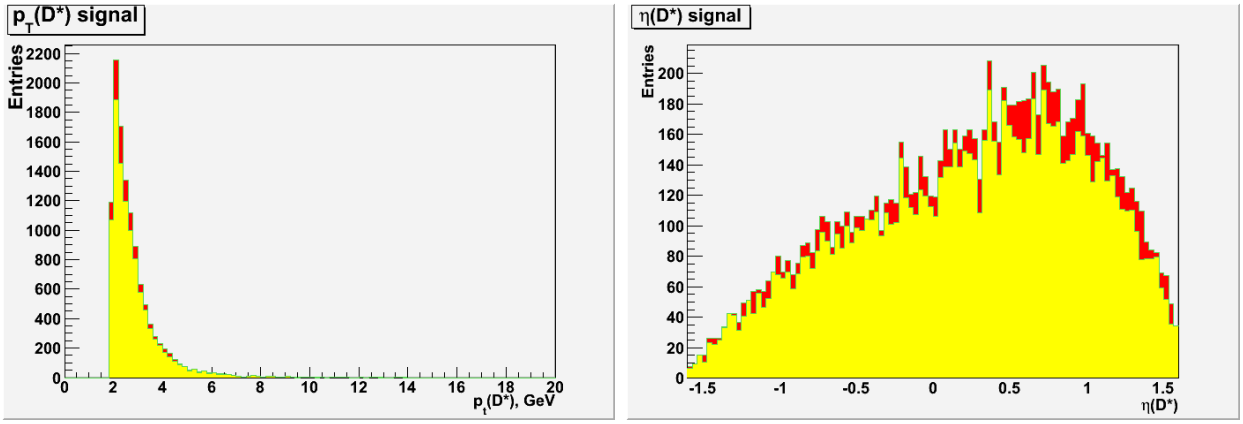

Figure 4.4: Comparison of distributions for $\eta(D*)$ and $p_T(D*)$ for LER (red-v07a, yellow-v06a).

0.5% larger statistics for MER, 4% for LER and 5% for HER. In new version appeared cuts for DCA: distance of closest approach of two helices or a helix and a point(in DSTAR blocks).

5 Comparison data with MC

The comparison between the data and MC distributions of $\eta(D*)$ and $p_T(D*)$ for all proton beam energies are shown in figure 4.1-4.3.

Discrepancies between data and Monte Carlo bigger than statistical error. To solve this problem we need to apply reweighting.

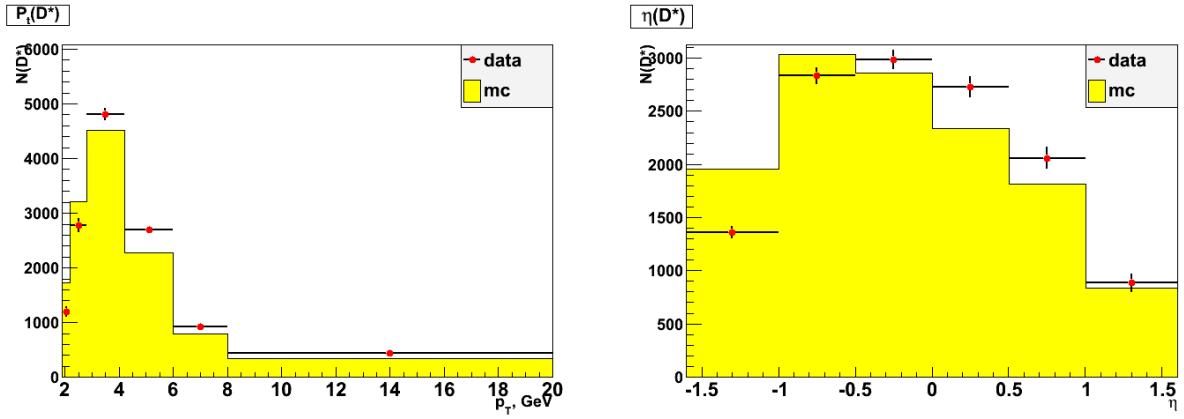

Figure 5.1: Control plots for $\eta(D*)$ and $p_T(D*)$ for HER (yellow - Monte Carlo).

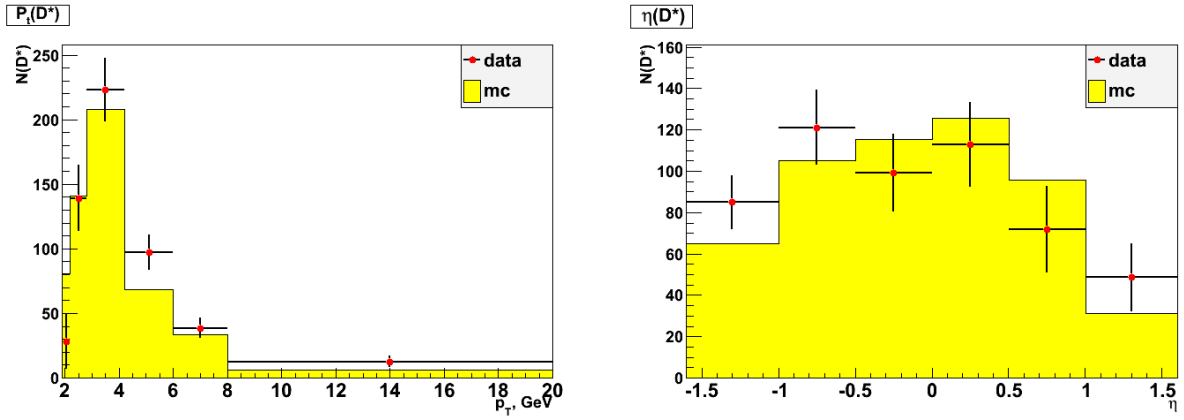

Figure 5.2: Control plots for $\eta(D*)$ and $p_T(D*)$ for MER (yellow - Monte Carlo).

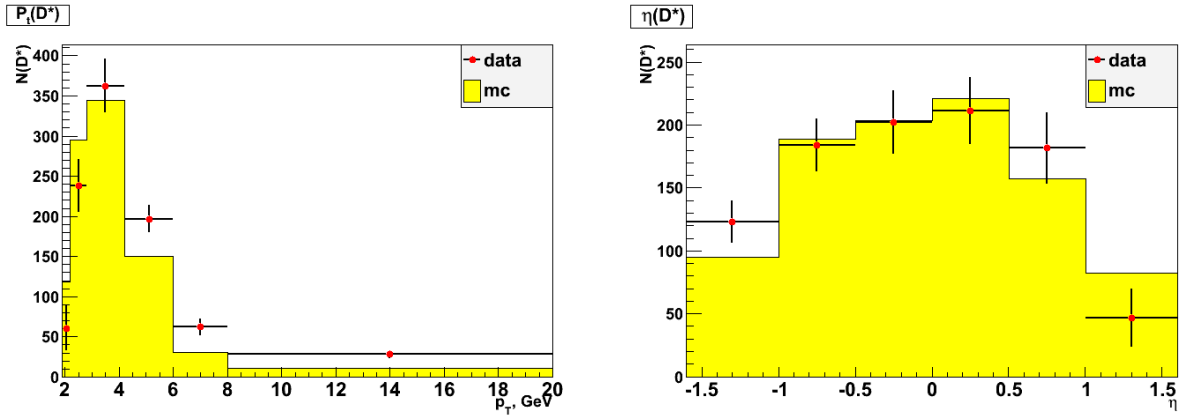

Figure 5.3: Control plots for $\eta(D*)$ and $p_T(D*)$ for LER (yellow - Monte Carlo).

6 Total cross section

The visible production cross section in ep collisions is calculated from the observed number of D^* mesons according to the formula

$$\sigma_{total}(D^*) = \frac{N^{data}_{reco}(D^*)}{L \cdot Br \cdot \alpha},$$

where L - the integrated luminosity;
$\alpha = \frac{N^{MC}_{reco}(D^*)}{N^{MC}_{true}(D^*)}$- acceptance;
$Br = 0.026$ - branching ratio;
$N^{data}_{reco}(D^*)$ - the number of reconstructed D^* mesons;
N^{MC}_{reco} - the number of reconstructed D^*, after passing through the detector, N^{MC}_{true} - the number of D^*, which were formed by the interaction (hadron level).

Energy dependence of total cross sections are presented in Figure 5.1.

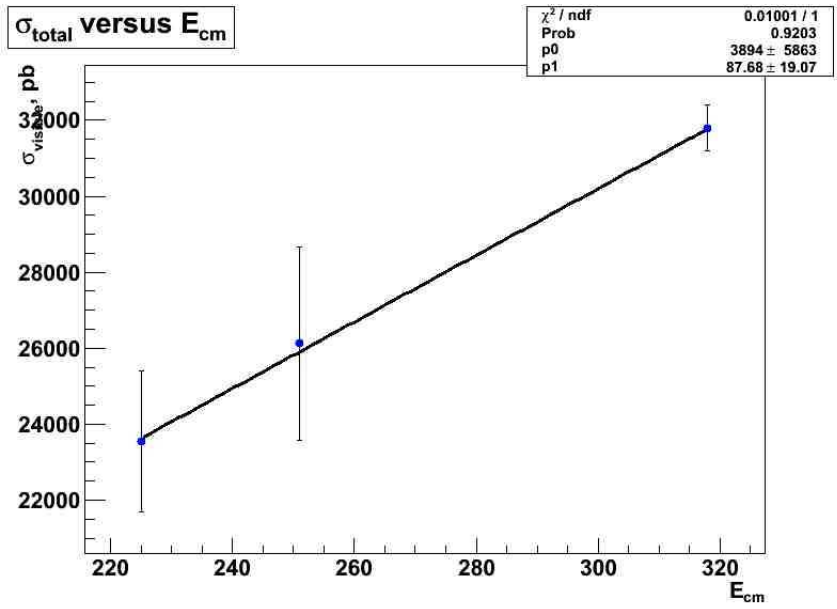

Figure 6.1: Energy dependence of total cross sections vs centre of mass.

The total cross sections for all proton beam energies are shown in the Table 3.

Table 4: Acceptance and total cross section.

E_p	$N(D^*)MC_{reco}$	$N(D^*)MC_{true}$	α	$\sigma_{total}(D^*), pb$
LER	461±24	3922	0.117 ±0.006	23536 ±1923
MER	417±22	4091	0.102 ±0.005	26127 ±26120
HER	13783 ±136	129278	0.107 ±0.001	31773 ±616

7 New D mesons Monte Carlo

The Pythia inclusive charm in photoproduction Monte Carlo sample with D^* filter for middle energy run (575 GeV) and low energy run (460 GeV) has a small statistics and same bugs. Therefore was prepared a new samples D mesons Monte Carlo for this periods with more statistics (4xDATA).

It is charm and beauty Monte Carlo samples for photoproduction:

- the MC-Samples were generated with PYTHIA v6.221 ;
- c and b production, full range of Q2;

Sample contains 8 D meson decay modes that includes all necessary backgrounds for D meson relevant analysis. Decay chains(for particles and antiparticles) for user code selection:

$D^{*+} \to D^0(\to \mathrm{K},\pi),pi_s$ with $p_t > 1.25$ GeV
$D^{*+} \to D^0(\to K_s,\pi,\pi),\pi_s$ with $p_t > 1.35$ GeV
$D^{*+} \to \mathrm{D}^0(\to \mathrm{K},\pi,\pi,\pi),\pi_s$ with $p_t > 2.3$ GeV
$D^0 \to \mathrm{K},\pi$ with $p_t > 2.6$ GeV
$D_s \to \phi(\to \mathrm{K},\mathrm{K}),\pi$ with $p_t > 1.7$ GeV
$D^+ \to \phi(\to \mathrm{K},\mathrm{K}),\pi$ with $p_t > 1.7$ GeV
$D^+ \to \mathrm{K},\pi,\pi$ with $p_t > 2.8$ GeV
$L_c \to \mathrm{K},\pi,\pi$ with $p_t > 2.8$ GeV

The necessary calculations for each process are shown in the Table 6.1, 6.2.

Data	Funnel Version	N Events	Process	Cross section,mb	Lumi,pb^{-1}	Reduction factor
07e$^+$ LER	num47t3.0	629234	CC dir	3,53*10^{-4}	57.5	~32
		457376	CG res	2.37*10^{-4}	53.26	~27
		64215	CP res	6.52*10^{-5}	52.35	~54
07e$^+$ MER	num57t3.0	414479	CC dir	3.95*10^{-4}	33.06	~32
		314393	CG res	2.61*10^{-4}	31.65	~26
		4600	CP res	7.65*10^{-5}	33.10	~56

Figure 7.1: Charm production.

Data	Funnel Version	N Events	Process	Cross section,mb	Lumi,pb^{-1}	Reduction factor
07e$^+$ LER	num47t3.0	18710	BB dir	$2.82*10^{-6}$	56.69	~8
		5900	BG res	$6.99*10^{-7}$	56.73	~7
		1600	BP res	$1,94*10^{-7}$	57.17	~7
07e$^+$ MER	num57t3.0	13368	BB dir	$3.42*10^{-6}$	31.8	~8
		4341	BG res	$8.57*10^{-7}$	32.39	~6
		1185	BP res	$2.48*10^{-7}$	35.05	~7

Figure 7.2: Beauty production.

After installing Orange were checked some a variable with MCDSTAR block (see Fig.6.3,6.4).

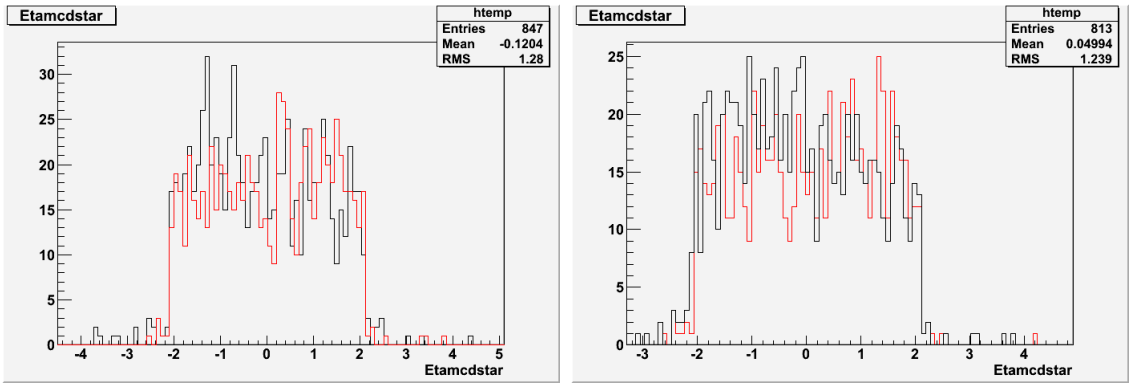

Figure 7.3: Distributions for ETAMCDSTAR block (red - direct process, black - resolved process).

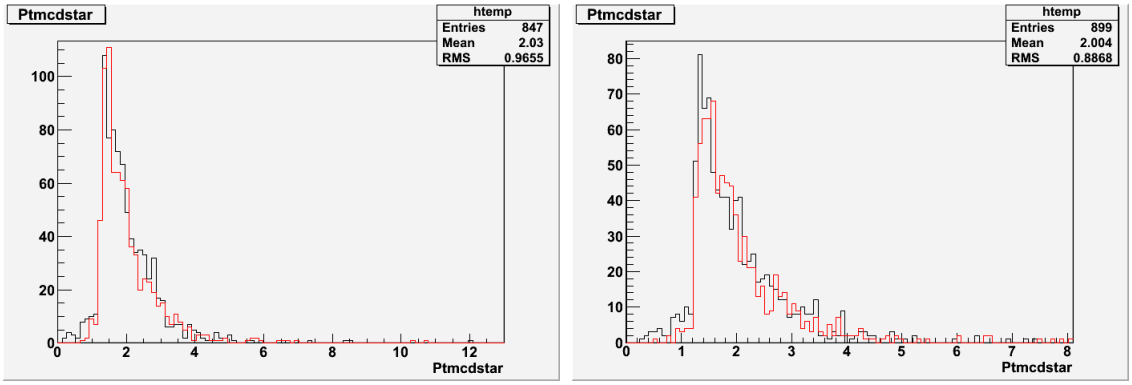

Figure 7.4: Distributions for PTMCDSTAR block (red - direct process, black - resolved process).

All together it makes 1177035 Events for LER, 1062159 Events for MER. More information and documentation at webpage [1].

8 Summary

In this analysis was study energy dependence of total cross section ratio and we can see, that total cross sections increase with energy.

- Acceptance and ratio of cross section calculated for different energy (HER, MER, LER).

- Was compating kinematic variables for different energies.

- The comparison of data with MC showed some discrepancies between data and Monte.

Compared new version Common Ntuples v07a with v06a for HER, MER, LER:

- the distributions of $\delta(M)$ and distributions of kinematic variables $p_T(D^*)$, $\eta(D^*)$ for MER, LER,HER;

- calculated the number of D^* mesons for v06a and v07a;

So, the distributions are similary. New version Common Ntuple has a litlle improve.

Was preapered a new samples D mesons Monte Carlo for MER and LER with lumi 4xDATA. The samples was send to funnel queue.

The energy dependence of total cross section presented in ZEUS collaboration at first.

References

[1] $http://www-zeus.desy.de/\ zaknat/DmesonMC/MCphp.html$

A Kinematic distributions for daughter particles D^*

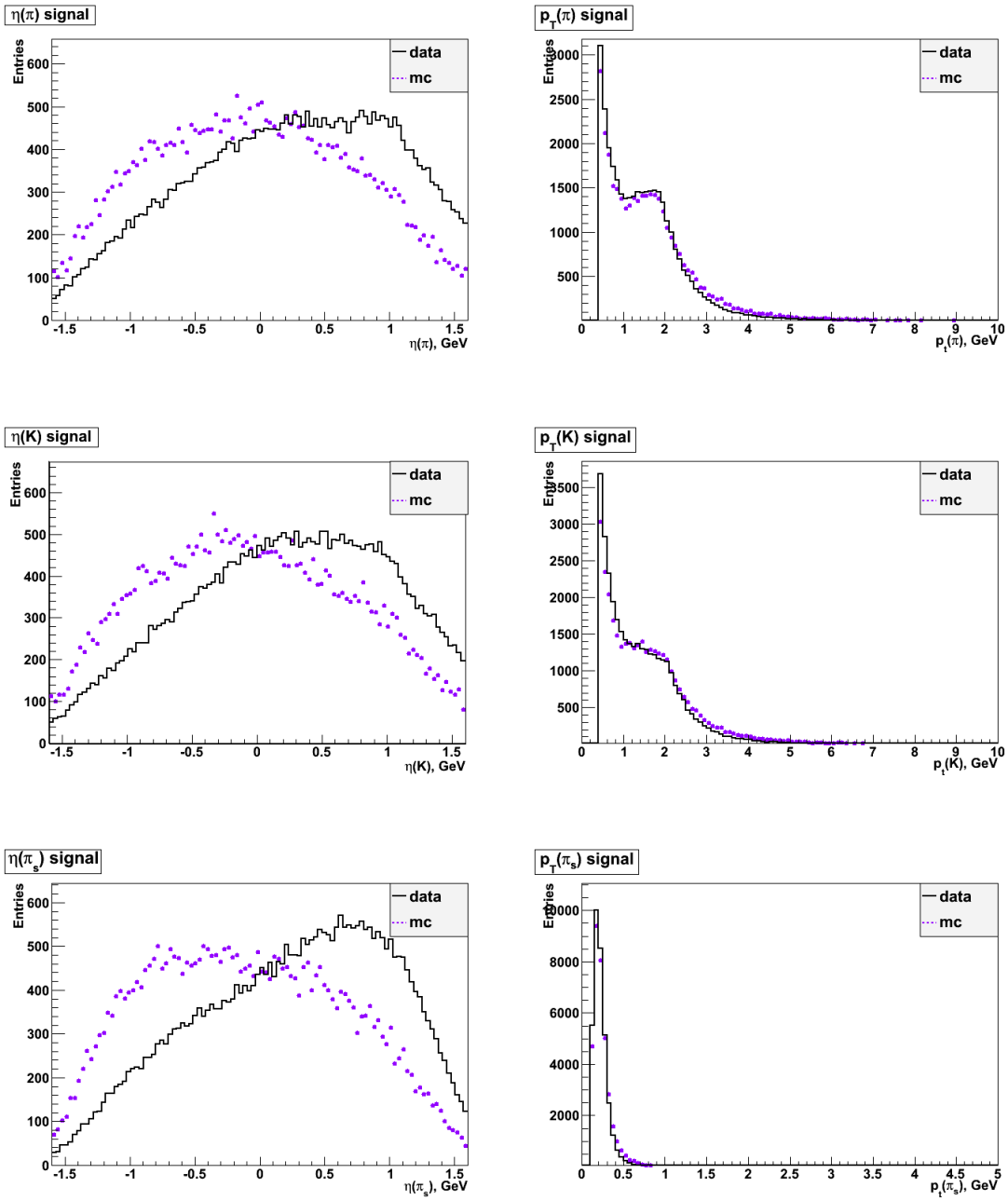

Figure A.1: Kinematic distributions for daughter particles D^* for HER (violet - MC)

B Control plots for π_s

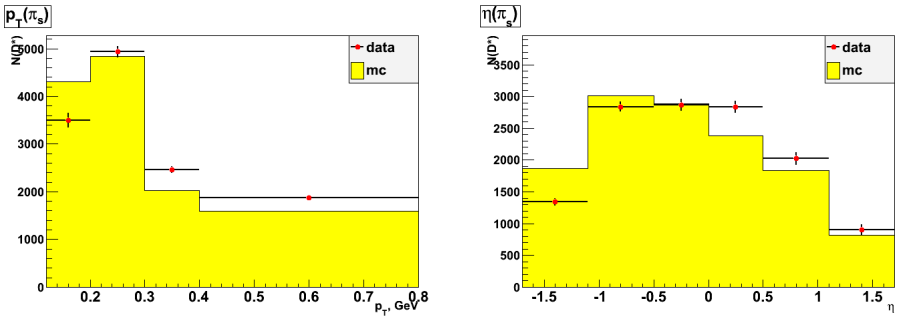

Figure B.1: Control plots for $\eta(\pi_s)$ and $p_T(\pi_s)$ for HER (yellow - Monte Carlo)

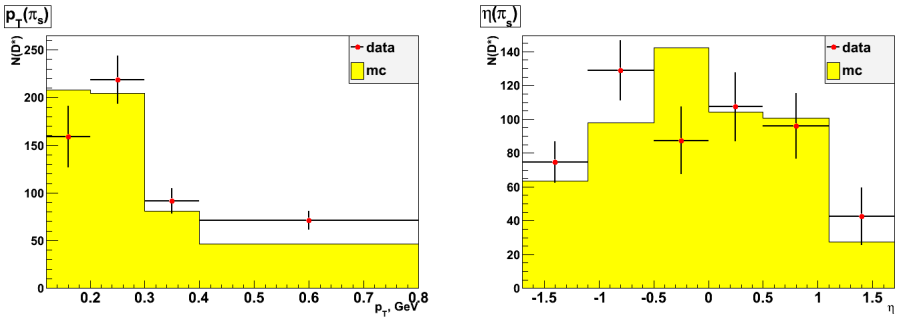

Figure B.2: Control plots for $\eta(\pi_s)$ and $p_T(\pi_s)$ for LER (yellow - Monte Carlo)

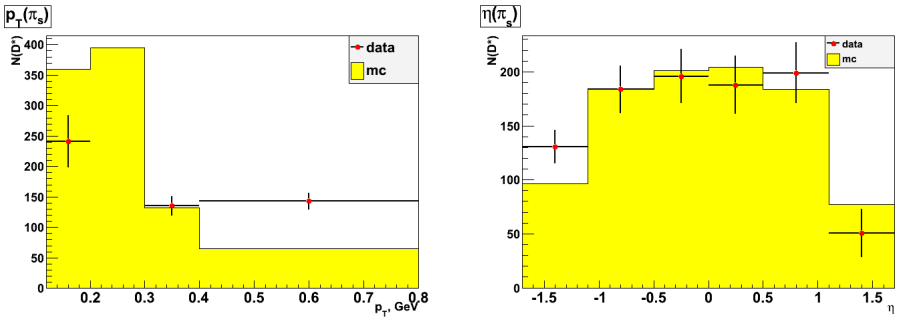

Figure B.3: Control plots for $\eta(\pi_s)$ and $p_T(\pi_s)$ for MER (yellow - Monte Carlo)

C Control plots for π

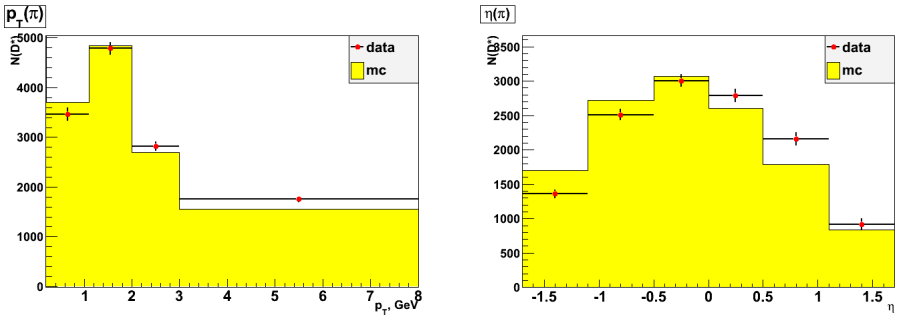

Figure C.1: Control plots for $\eta(\pi)$ $p_T(\pi)$ for HER (- Monte Carlo)

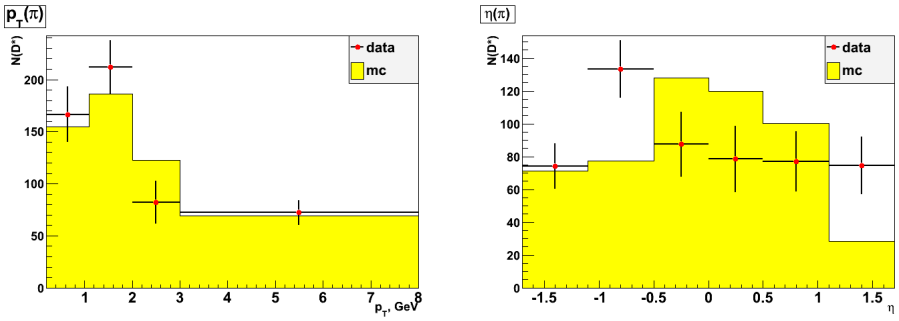

Figure C.2: Control plots for $\eta(\pi)$ $p_T(\pi)$ for LER (- Monte Carlo)

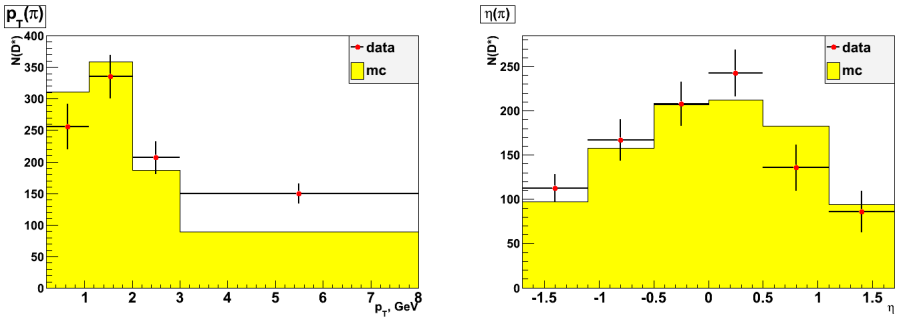

Figure C.3: Control plots for $\eta(\pi)$ $p_T(\pi)$ for MER (- Monte Carlo)

D Control plots for K

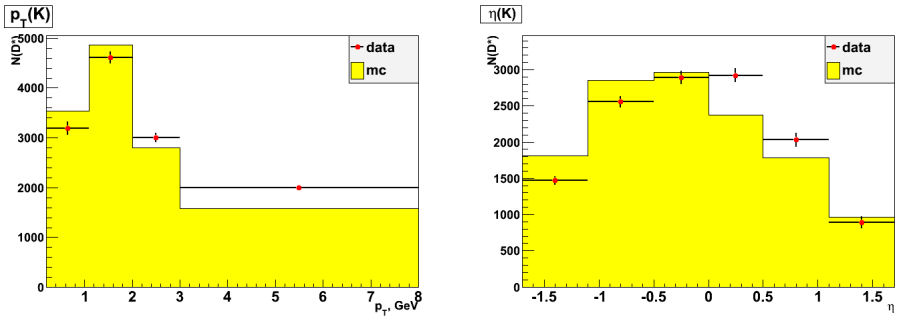

Figure D.1: Control plots for $\eta(K)$ $p_T(K)$ for HER (- Monte Carlo)

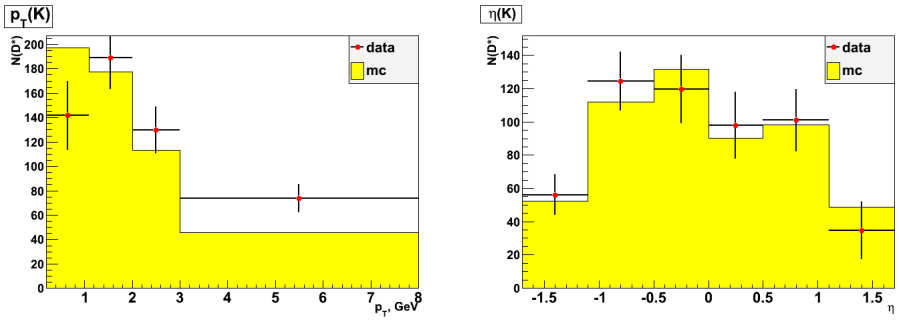

Figure D.2: Control plots for $\eta(K)$ $p_T(K)$ for LER (- Monte Carlo)

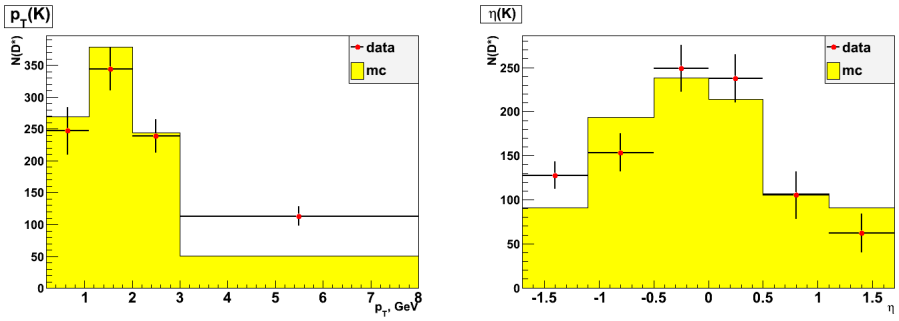

Figure D.3: Control plots for $\eta(K)$ $p_T(K)$ for MER (- Monte Carlo)

E Energy dependence for ratio of total cross section

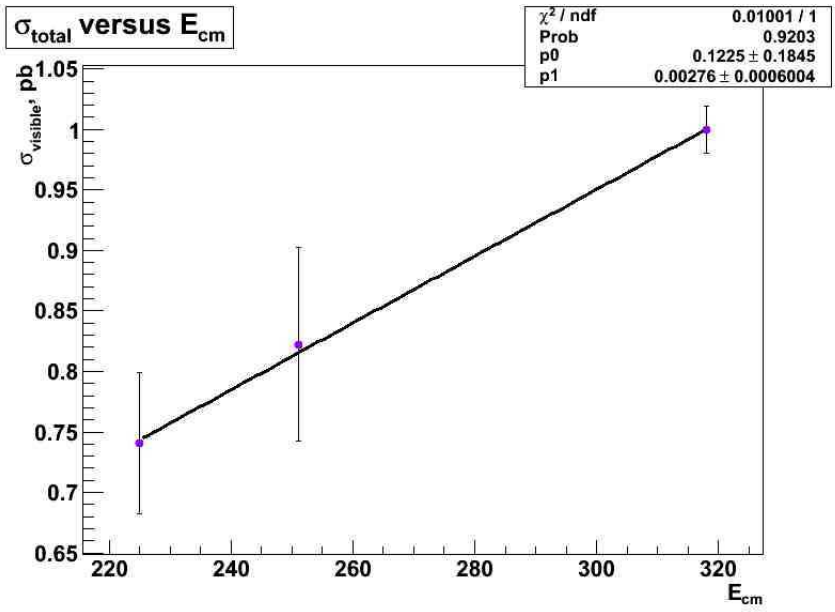

Figure E.1: Energy dependence for ratio of total cross section